

# Electron Mobility Model for $\langle 110 \rangle$ Stressed Si Including Strain-Dependent Mass

S. Dhar, E. Ungersboeck, H. Kosina, T. Grasser, and S. Selberherr

Institute for Microelectronics, TU Vienna, Gusshausstrasse 27–29/E360, 1040 Vienna, Austria

E-mail: dhar@iue.tuwien.ac.at

## I. ABSTRACT

Stress induced enhancement of electron mobility has primarily been attributed to the splitting of the conduction bands. However, experiments [1] have indicated that the mobility enhancement cannot solely be attributed to this effect, and a recent study has shown that a stress along the  $\langle 110 \rangle$  direction leads to a change of the effective mass [2]. This work investigates the effect of the variation of the effective mass with stress along  $\langle 110 \rangle$  direction on the electron mobility. An improved low-field mobility model incorporating the effective mass change is presented.

## II. INTRODUCTION

The band structure (BS) of Si including the effect of stress/strain has been calculated using the empirical non-local pseudopotential method (EPM) [3]. For stress along  $\langle 110 \rangle$ , the effect of the internal displacement of the atoms [4] has been taken into account in the BS calculations. The effective masses for the two-fold degenerate  $\Delta_2$ -valleys and the four-fold degenerate  $\Delta_4$ -valleys were extracted from the BS data using curve fitting. Fig. 1 depicts the variation of the two transversal ( $m_{t\parallel}$ ,  $m_{t\perp}$ ) and the longitudinal ( $m_l$ ) masses for the  $\Delta_2$ -valleys as a function of the strain for different values of the internal displacement parameter,  $\xi$ . The variation of  $m_{t\parallel}$ ,  $m_{t\perp}$ , and  $m_l$  has been fitted using a quadratic function of the stress. Fig. 1 shows that there is a significant change in  $\Delta m^*$  for increasing strain along  $\langle 110 \rangle$  which translates into a mobility variation as shown in Fig. 2. Also shown in Fig. 3 is the splitting,  $\Delta\epsilon$  for biaxially/uniaxially strained Si. It is observed that biaxial tension is more effective in splitting the conduction bands than  $\langle 110 \rangle$  uniaxial tension.

## III. MODELING

The mobility tensor for a stress along  $\langle 110 \rangle$  can be calculated analytically using an expression proposed in [5]. It includes the effect of strain-induced splitting of

the conduction band valleys in Si, inter-valley scattering, doping dependence and temperature dependence. The model however assumes a constant  $m_t$  and  $m_l$  in Si. Band structure calculations show that for a uniaxial tensile stress along  $\langle 110 \rangle$ , the two-fold degenerate  $\Delta_2$ -valleys, which are lowered in energy, experience a change in the effective masses. This results in a pronounced anisotropy of the mobility in the transport plane (see Fig. 4). For uniaxial compression, however, there is a negligible change in the effective masses of the lowered four fold degenerate  $\Delta_4$ -valleys. We have therefore extended the model in [5] to account for the variation of the effective mass of the  $\Delta_2$ -valleys with stress for uniaxial tensile stress. This in turn leads to a modification of the scaled inverse mass tensor  $\hat{m}_z^{-1}$  (Eq. (6) in [5]), which is obtained as shown below.

$$\hat{m}_z^{-1} = m_c \begin{pmatrix} m_t^{-1} & m_\Delta^{-1} & 0 \\ m_\Delta^{-1} & m_t^{-1} & 0 \\ 0 & 0 & m_l^{-1} \end{pmatrix} \begin{matrix} m_t^{-1} = (m_{t\parallel}^{-1} + m_{t\perp}^{-1})/2 \\ m_\Delta^{-1} = (m_{t\parallel}^{-1} - m_{t\perp}^{-1})/2 \\ m_c^{-1} = (m_{t\parallel}^{-1} + m_{t\perp}^{-1} + m_l^{-1})/3 \end{matrix}$$

Here  $m_c$  and  $m_t$  denote the average conductivity and transversal mass respectively. The  $m_{t\parallel}$  and  $m_{t\perp}$  denote respectively the transversal masses along  $\langle 110 \rangle$  and  $\langle \bar{1}10 \rangle$  of the  $\Delta_2$ -valleys. The mobility tensor thus calculated using  $\hat{m}_z^{-1}$  becomes non-diagonal in the principal coordinate system. Fig. 5 and Fig. 6 show a comparison of the variation of the electron mobility components with increasing stress as obtained from Monte Carlo simulations and the analytical model. A good agreement is obtained.

This work has been partly supported by the European Commission, project D-DOT FET, 012150-2.

## REFERENCES

- [1] K. Uchida et al., IEDM, pp. 229–232 (2004).
- [2] H. Irie et al., IEDM, pp. 225–228 (2004).
- [3] M.M. Rieger and P. Vogl, Phys. Rev. B, 48 (19), 14276, 1993.
- [4] C. G. Van de Walle, Phys. Rev. B, 34 (8), 5621–5633, 1986.
- [5] S. Dhar et al., IEEE Trans. ED, vol. 52, pp. 527–533 (2005).

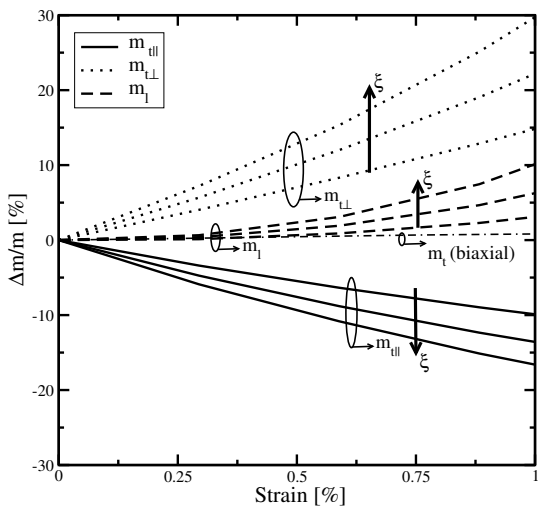


Fig. 1. Effect of the uniaxial  $\langle 110 \rangle$  tensile strain on the transversal and longitudinal masses of the  $\Delta_2$ -valleys ( $\xi = 0, 0.53, 1.0$ ).

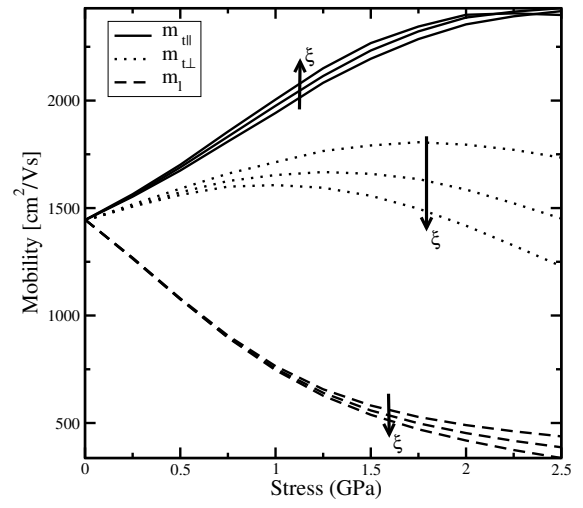


Fig. 2. Mobility as a function of tensile stress with internal displacement as a parameter ( $\xi = 0, 0.53, 1.0$ ).

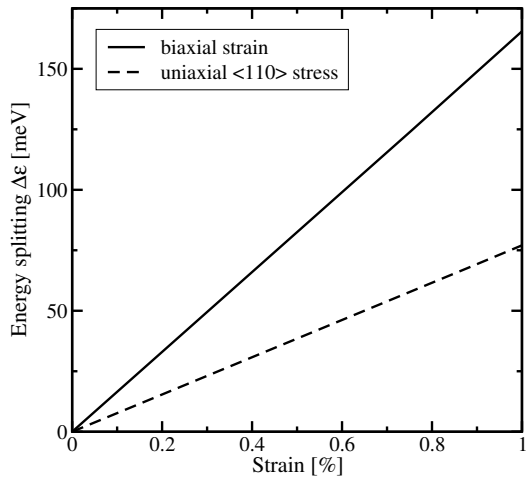


Fig. 3. Effect of biaxial tensile strain and uniaxial  $\langle 110 \rangle$  tensile stress on valley splitting. Strain component in the stressed direction is plotted.

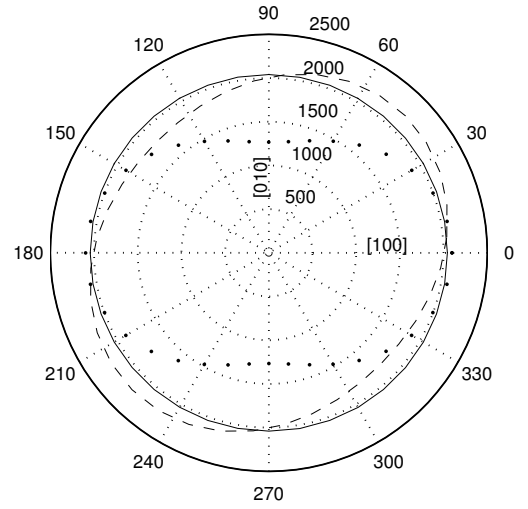


Fig. 4. Variation of the in-plane mobility with in-plane angle for uniaxial  $\langle 110 \rangle$  and  $\langle 110 \rangle$  tensile stress. solid:  $\langle 110 \rangle$  without mass correction; dashed:  $\langle 110 \rangle$  with mass correction; dotted: uniaxial  $\langle 100 \rangle$  stress.

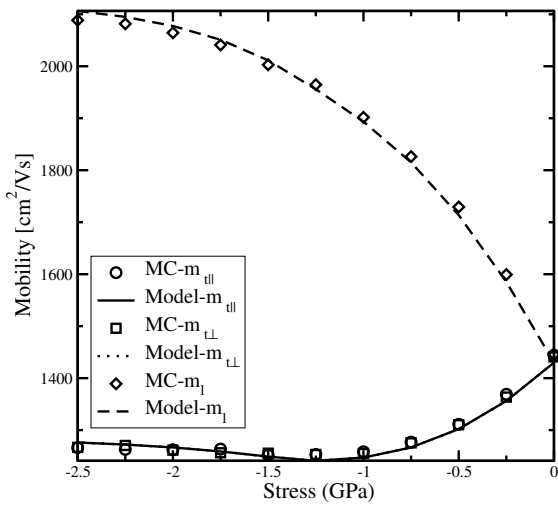


Fig. 5. Comparison of electron mobility components obtained from the MC simulations and the analytical model for uniaxial  $\langle 110 \rangle$  compressively strained Si. Here  $m_{r||} = m_{r\perp}$ .

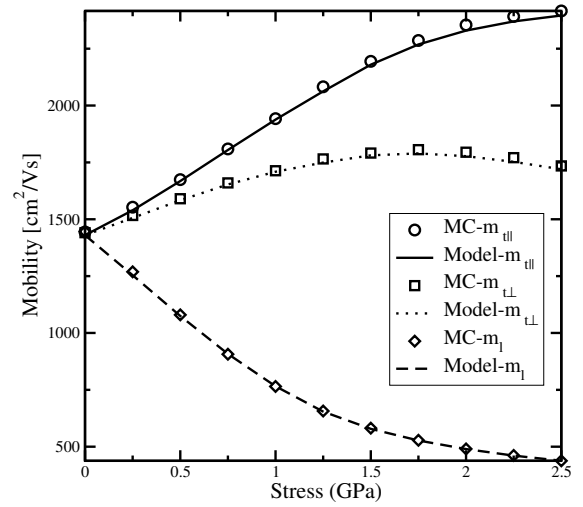


Fig. 6. Comparison of electron mobility components obtained from the MC simulations and the analytical model for uniaxial  $\langle 110 \rangle$  tensile strained Si.